Supporting Information for

Twist Angle has Weak Influence on Charge Separation and Strong Influence on Recombination in MoS_2/WS_2 Bilayer: Ab Initio Quantum Dynamics

Yonghao Zhu,[1] Wei-Hai Fang,[1] Angel Rubio,[2] Run Long,[1*] Oleg V. Prezhdo[3]

[1]*College of Chemistry, Key Laboratory of Theoretical & Computational Photochemistry of Ministry of Education, Beijing Normal University, Beijing, 100875, People's Republic of China*

[2]*Max Planck Institute for the Structure and Dynamics of Matter, 22761 Hamburg, Germany*

[3]*Departments of Chemistry, and Physics and Astronomy, University of Southern California, Los Angeles, CA 90089, USA*

1. Moiré superlattices

The Moiré superlattices of bilayer graphene have been studied widely in the recent years.[1, 2] Monolayer transition metal dichalcogenides (TMDs) are similar to graphene in both direct and reciprocal lattice vector spaces. Therefore, the Moiré superlattices of TMD junctions can be constructed using similar methods without additional strain for two single layers.[3] The possible angles (θ) can be calculated by the following formula:[1, 2]

$$\cos(\theta_i) = \frac{3*i^2+3*i+1/2}{3*i^2+3*i+1} \quad i = 0, 1, 2, 3\ldots$$

The supercell vectors are:

$$\vec{A} = i*\vec{a} + (i+1)*\vec{b}$$

$$\vec{B} = -(i+1)*\vec{a} + (2*i+1)*\vec{b}$$

where $\vec{a}$ and $\vec{b}$ are the unit cell lattice vectors. The lattice constant of the supercell is:

$$L = \sqrt{3*i^2+3*i+1}*a_0$$

* Corresponding author, E-mail: runlong@bnu.edu.cn

where a_0 is the lattice constant of the unit cell. ***Table S1*** shows that larger *i* can produce smaller twist angles and bigger superlattices. Considering the Moiré pattern and the superlattice size, we build structures with the twist angles of 9.43° (*i*=3, relative to 0°) and 50.57° (*i*=3, relative to 60°). ***Figure S1*** shows the Moiré patterns in these superlattices.

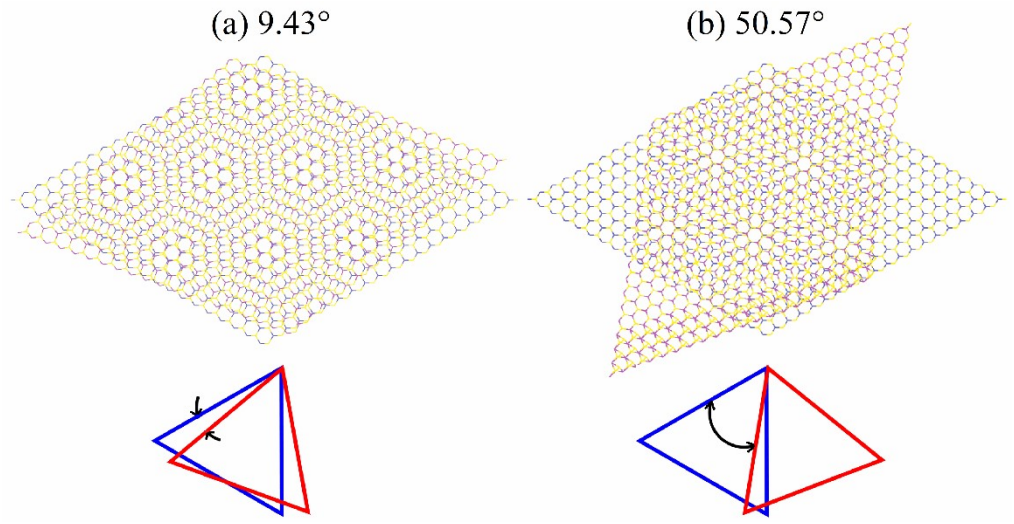

Figure S1. Moiré patterns in the twisted 9.43° and 50.57° TMD heterojunctions.

2. Reciprocal space and k-point unfolding

Interpretation of simulation results performed with superlattices benefits from the zone folding analysis. Popescu et al.[4, 5] provided a method to analyze the effective band structure. The direct superlattice can be calculated by the following formula:

$$DT_{supercell} = tm \cdot DT_{primitive-cell}$$

where $DT_{supercell}$ and $DT_{primitive-cell}$ are the direct lattice vectors of the supercell and the primitive cell, respectively, and tm is the transition matrix. The reciprocal lattice vectors, $RT_{primitive-cell}$ and $RT_{supercell}$, can be obtained by:

$$RT_{supercell} = (tm^T)^{-1} \cdot RT_{primitive-cell}$$

The k-points folding can be obtained by:

$$k_{supercell} = k_{primitive-cell} \cdot tm^T$$

where $k_{supercell}$ and $k_{primitive-cell}$ are the k-point coordinates in the supercell and the primitive

cell. For example, the direct bandgap of monolayer MoS_2 is at the K-point (***Fig. S2a***). For the 3*3 supercell, the K-point, $(1/3\ 1/3)$, will be folding to the Γ-point, $(0\ 0)$. For the supercells of 0° and 60° (***Fig. 1a*** and ***Fig. 1b***), $tm = \begin{pmatrix} 7 & 3 \\ -3 & 4 \end{pmatrix}$, such that $K_{supercell} = (1/3\ 1/3)$.

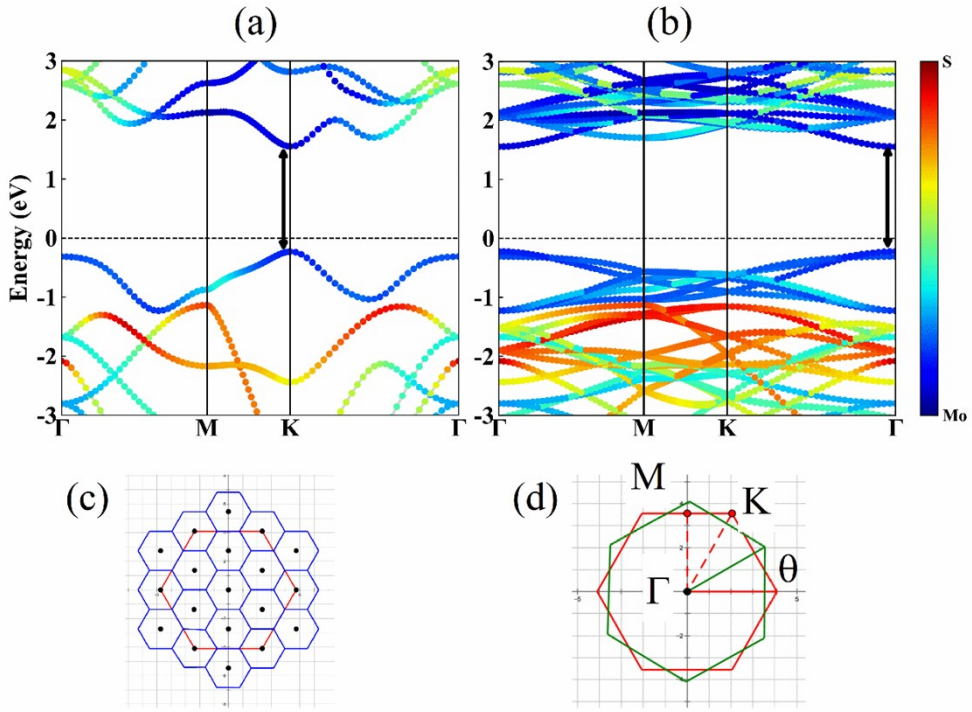

Figure S2. Monolayer MoS_2 band structures of **(a)** unit cell and **(b)** 3*3*1 supercell. **(c)** K-point folding for the 3*3*1 supercell. The red and blue lines represent the first Brillouin zones of the primitive and 3*3*1 supercells, respectively. The black dots are the Γ-points. **(d)** Twist angle in the reciprocal space. The dark green lines show twist of the first Brillouin zone.

Table S1. Twist Angle and Superlattice Size

i	Twist Angle	Superlattice	i	Twist Angle	Superlattice
0	60°	1	5	6.01°	√91
1	21.79°	√7	6	5.09°	√127
2	13.17°	√19	7	4.41°	√169
3	9.43°	√37	8	3.89°	√217
4	7.34°	√61	9	3.48°	√271

3. Hole transfer and recombination at the K-point

The bilayer TMD junctions show indirect band gap, generally, owing to strong interlayer coupling. ***Fig. S3a*** shows the band structure for the 3R stacking, indicating that the VBM is located at the Γ-point, and the CBM is located at the K-point. However, the direct bandgap is the smallest at the K-point. The charge density of the VBM at the Γ-point does not localize on either layer. According to the contributions of the charge densities at the K-point, MoS_2/WS_2 vdWHs present type-II alignment with the VBM and CBM of WS_2 lying higher than those of MoS_2. The G_0W_0 plus Bethe-Salpeter calculation confirms charge separation in the MoS_2/WS_2 vdWH. Furthormore, the oscillator strength of the interlayer exciton is larger than that of the intarlayer exciton.[6] A variety of channels are available for interlayer charge recombination in TMD vdWHs, including recombination between K-K, K-Γ, Q-K, and Q-Γ k-points. However, K-K recombination is the dominant pathway, because the other channels are momentum forbidden. Okada et al.[7] indicate that the K-K recombination is faster than K-Γ and Q-Γ recombination. K-K exciton properties have been widely studied in TMD vdWHs.[7-18] The current study focuses on the dominant K-K exciton recombination channel.

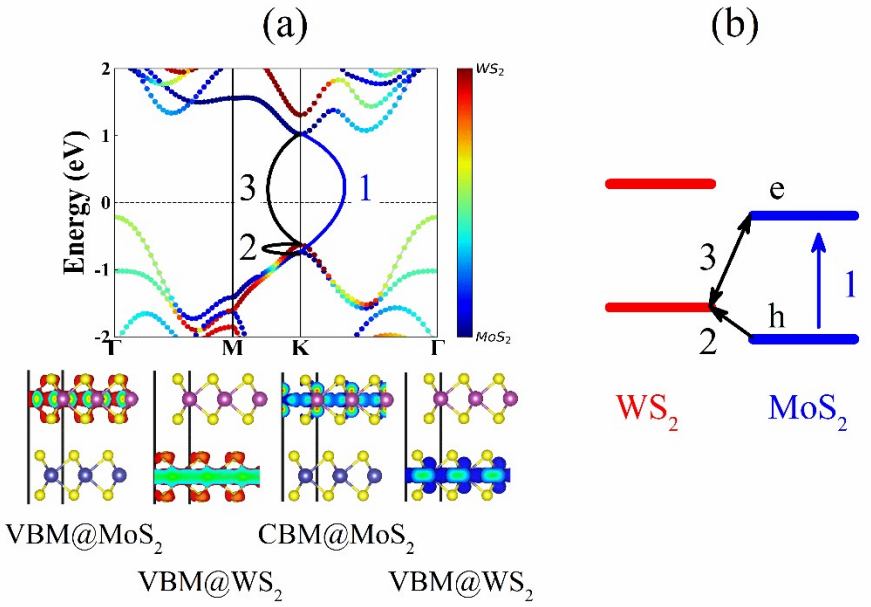

Figure S3. Unit cell of the MoS_2/WS_2 vdWH. **(a)** Band structure, and the VBM and CBM charge densities at the K-point. **(b)** Type-II band alignment. The processes 1, 2 and 3 represent initial photoexcitation, hole transfer, and K-K recombination, respectively.

4. Layer projected density of states

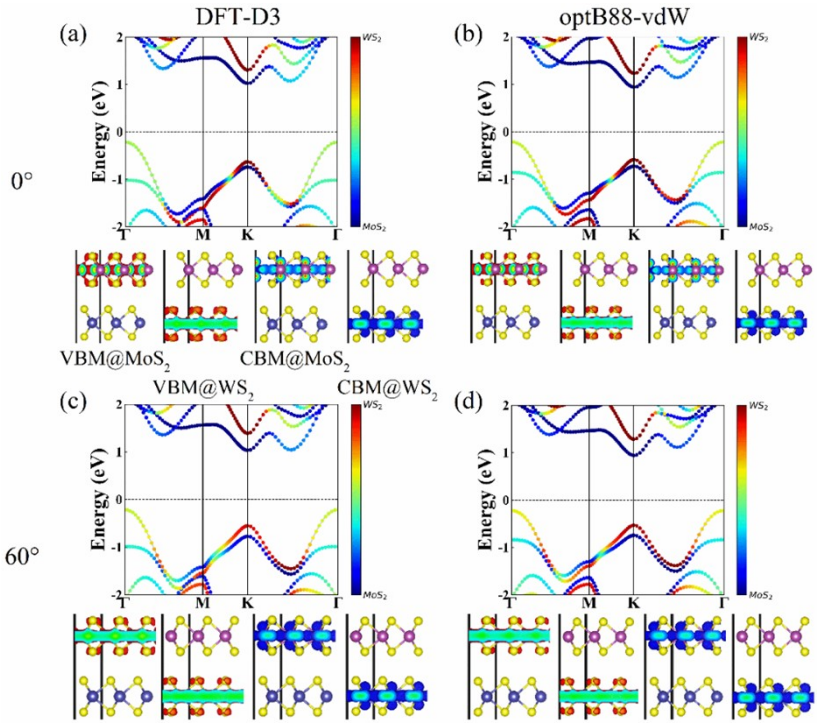

Figure S4. Band structure and the CBM and VBM charge densities of the MoS_2/WS_2 heterojunction with the 0° and 60° twist angles calculated using (a, c) DFT-D3 and (b, d) optB88-vdW functionals.

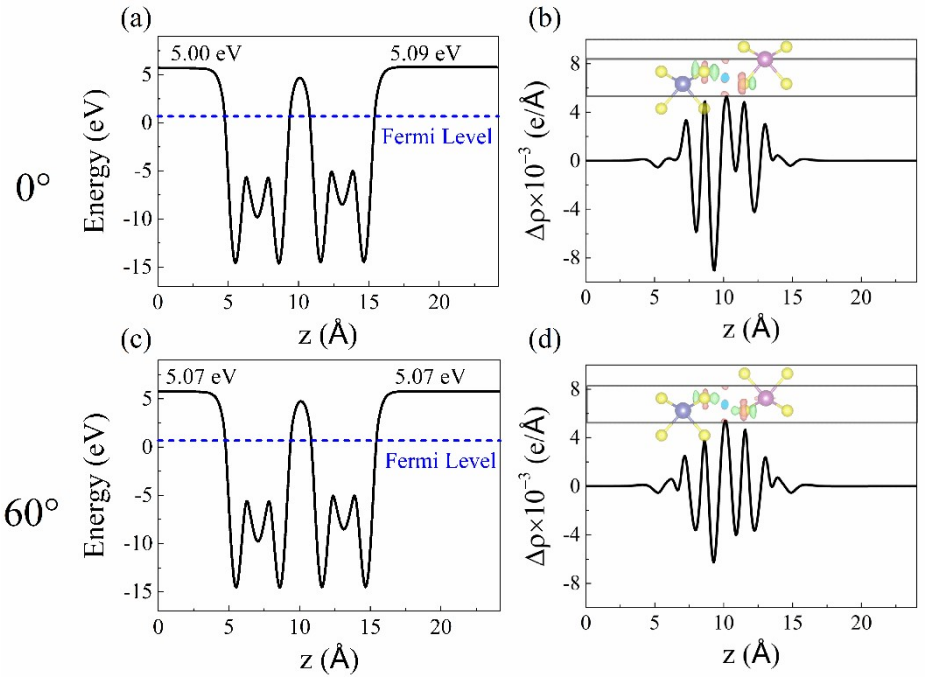

Figure S5. (a, c) Work functions and (b, d) planar-averaged charge density differences in the MoS_2/WS_2 heterojunctions with (a, b) 0° and (c, d) 60° twist angles.

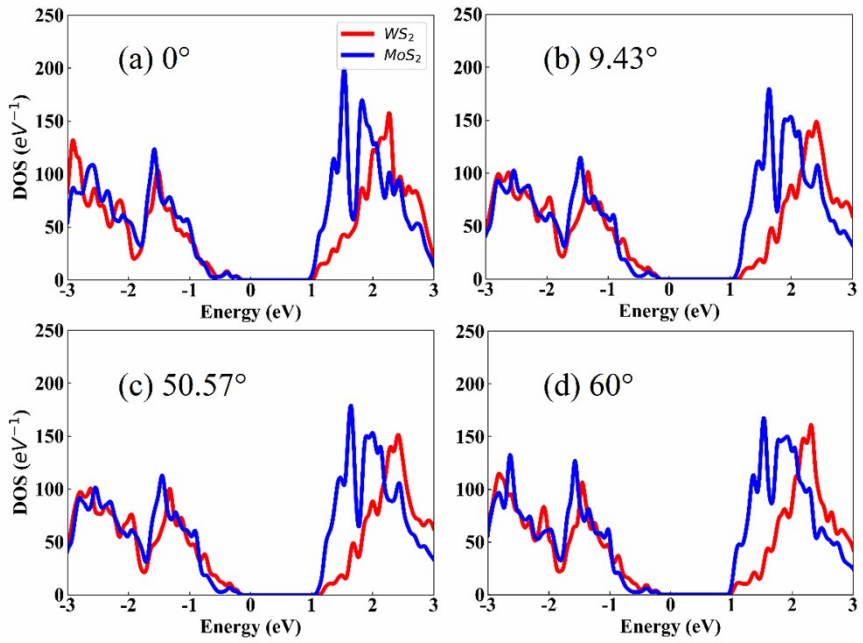

Figure S6. Layer projected density of states (DOS) of the MoS_2/WS_2 vdWHs.

5. Evolution of Kohn-Sham orbital energies

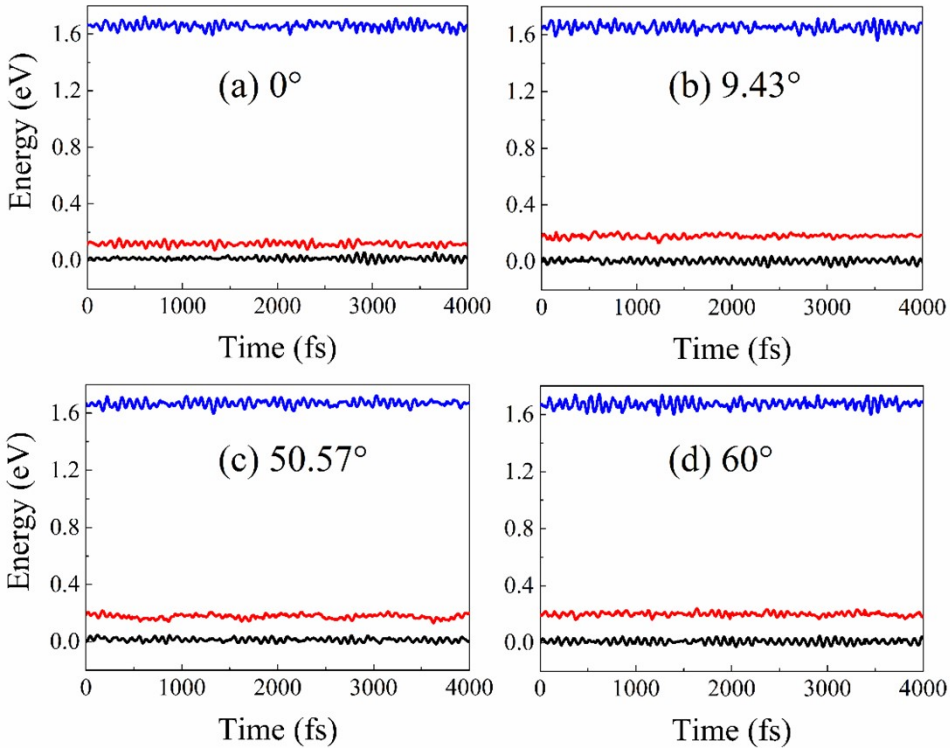

Figure S7. Evolution of the energies of VBM@MoS_2 (black lines), VBM@WS_2 (red lines), and CBM@MoS_2 (blue lines) at the K-point.

6. Fitting the electron-hole recombination NA-MD results

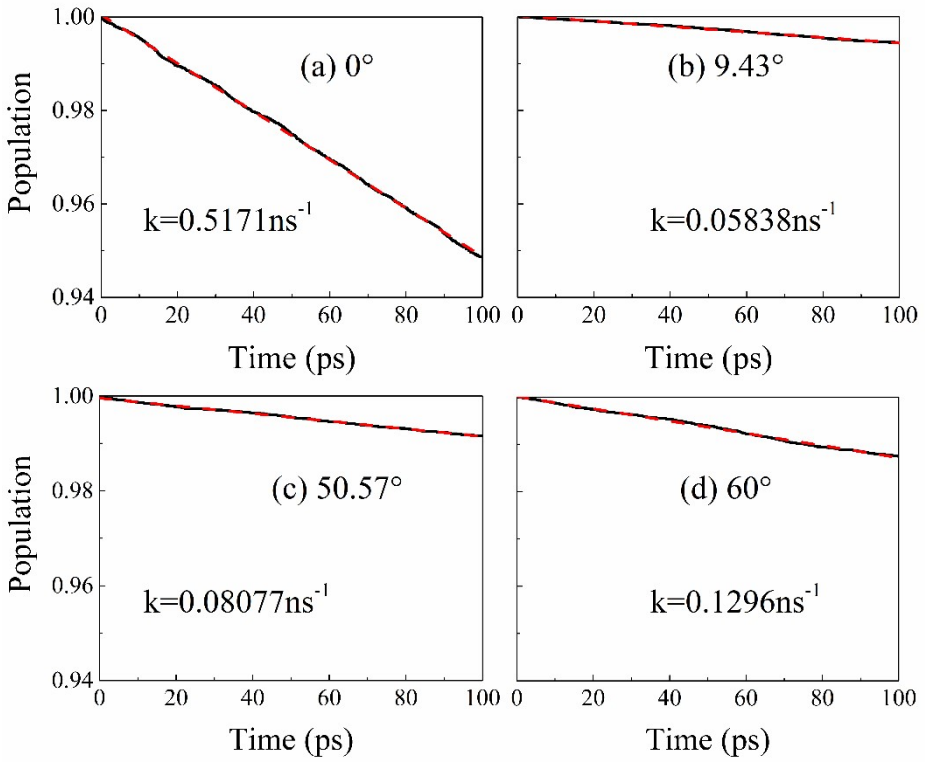

Figure S8. Fitting of the short-time nonradiative electron-hole recombination in the MoS_2/WS_2 vdWHs using linear functions.

References:

1. S. Shallcross, S. Sharma and O. A. Pankratov, *J. Phys.: Condens. Matter*, 2008, **20**, 454224.
2. J. M. B. Lopes dos Santos, N. M. R. Peres and A. H. Castro Neto, *Phys. Rev. Lett.*, 2007, **99**, 256802.
3. M. R. Rosenberger, H.-J. Chuang, M. Phillips, V. P. Oleshko, K. M. McCreary, S. V. Sivaram, C. S. Hellberg and B. T. Jonker, *ACS Nano*, 2020, **14**, 4550-4558.
4. V. Popescu and A. Zunger, *Phys. Rev. Lett.*, 2010, **104**, 236403.
5. V. Popescu and A. Zunger, *Phys. Rev. B*, 2012, **85**, 085201.
6. E. Torun, H. P. C. Miranda, A. Molina-Sánchez and L. Wirtz, *Phys. Rev. B*, 2018, **97**, 245427.
7. M. Okada, A. Kutana, Y. Kureishi, Y. Kobayashi, Y. Saito, T. Saito, K. Watanabe, T. Taniguchi, S. Gupta, Y. Miyata, B. I. Yakobson, H. Shinohara and R. Kitaura, *ACS Nano*, 2018, **12**, 2498-2505.
8. H. Yu, G.-B. Liu and W. Yao, *2D Mater.*, 2018, **5**, 035021.
9. R. Gillen and J. Maultzsch, *Phys. Rev. B*, 2018, **97**, 165306.
10. B. Miller, A. Steinhoff, B. Pano, J. Klein, F. Jahnke, A. Holleitner and U. Wurstbauer, *Nano Lett.*, 2017, **17**, 5229-5237.
11. J. R. Schaibley, P. Rivera, H. Yu, K. L. Seyler, J. Yan, D. G. Mandrus, T. Taniguchi, K. Watanabe, W. Yao and X. Xu, *Nat. Commun.*, 2016, **7**, 13747.
12. M. Brotons-Gisbert, H. Baek, A. Campbell, K. Watanabe, T. Taniguchi and B. D. Gerardot, *arXiv reprints*, 2021, arXiv:2101.07747.

13. C. Jin, J. Kim, M. I. B. Utama, E. C. Regan, H. Kleemann, H. Cai, Y. Shen, M. J. Shinner, A. Sengupta, K. Watanabe, T. Taniguchi, S. Tongay, A. Zettl and F. Wang, *Science*, 2018, **360**, 893.
14. T. Li, T. Yu, X. Cui, K. Zhang, J. Liu, Q. Meng, H. Cai, N. Pan, B. Wang, Z. Dong and X. Wang, *arXiv reprints*, 2019, arXiv:1903.06899.
15. L. Yuan, B. Zheng, J. Kunstmann, T. Brumme, A. B. Kuc, C. Ma, S. Deng, D. Blach, A. Pan and L. Huang, *Nat. Mater.*, 2020, **19**, 617-623.
16. T. Deilmann and K. S. Thygesen, *Nano Lett.*, 2018, **18**, 1460-1465.
17. H. Zhu, J. Wang, Z. Gong, Y. D. Kim, J. Hone and X. Y. Zhu, *Nano Lett.*, 2017, **17**, 3591-3598.
18. J. Kim, C. Jin, B. Chen, H. Cai, T. Zhao, P. Lee, S. Kahn, K. Watanabe, T. Taniguchi, S. Tongay, M. F. Crommie and F. Wang, *Sci. Adv.*, 2017, **3**, e1700518.